ELSEVIER

International Journal of Minerals, Metallurgy and Materials
Volume 16, Number 5, October 2009, Page 525

Materials

Effects of solution environments under disbonded coatings on the corrosion behaviors of X70 pipeline steel in acidic soils

Xu Chen[1,2], *Cui-wei Du*[1], *Xiao-gang Li*[1], *Chuan He*[2], *Ping Liang*[1], *and Lin Lu*[1]

1) School of Materials Science and Engineering, University of Science and Technology Beijing, Beijing 100083, China
2) School of Storage and Architecture Engineering, Liaoning Shihua University, Fushun 113001, China
(Received 2008-06-09)

Abstract: A rectangle crevice assembly was used to study the effects of cathodic protection (CP) potential, crevice thickness, holiday size, bubbling CO_2, and surface condition on the chemical and electrochemical environment of the local solution under disbonded coatings. It is found that the cathodic protection removes dissolved oxygen from the crevice and thus shifts the solution to a more alkaline state. Furthermore, the potential of the steel reaches the protected potential range. The available protection distance increases with the negative applying potential. The steady potential and pH distribution are easily achieved, but the polarization degree is not satisfied within the thinner crevice. The difference in the solution environment is found to correlate to the holiday size. The smaller the holiday, the smaller the difference is. The presence of CO_2 inhibits the formation of an alkaline environment. It is also found that the rust layer dramatically decreases the polarization rate in the crevice.

Key words: pipeline steel; polarization; cathodic protection; crevice corrosion

[*This work was financially supported by the National Science & Technology Infrastructure Development Program of China (No.2005DKA10400).*]

1. Introduction

It is common to combine the applications of coating and cathodic protection (CP) to protect buried steel pipelines. The coating provides a barrier between the environments and the pipeline steel, and thus protects the steel from corrosion. However, pinholes and ruptures, called holidays, can be formed from either a faulty coating application process, or mechanical damage that occurs either during or after pipeline installation. The development of holiday leads to the loss of adhesion between the pipe and coating in the surrounding area. Water in the soil can then flow through the holiday and into the crevice between the pipe and disbonded coating, which leads to pipe surface corrosion [1-2]. In several instances, the cathodic protection lacks the ability to mitigate the corrosion under disbonded coating, especially in the low-conductance soil. This inability of cathodic protection to lessen corrosion is primarily because of the fact that extra cathodic protection cannot provide enough current to the holidays. Generally, it is thought that the coating acts as a shield against the cathodic protection current [3]. The cathodic current must be able to penetrate into the holidays in order to polarize the steel to a potential of more than –0.85 V *vs*. the cooper-cooper sulfate electrode (CSE). However, the high potential drop of the solution results in the cathodic protection invalidated within the crevice. The reduce reaction of O_2 or H_2O can generate alkaline environment under the disbonded coating. A sensitive potential and pH range of stress corrosion cracking (SCC) are obtained [4-9]. However, overprotection is not advisable owing to H_2 evolution on the surface of the pipes. The enrichment of hydrogen atoms on the surface can result in hydrogen brittleness [10-14]. The electrochemical reaction caused by the cathodic oxygen or water reduce reaction can generate OH^-. The alkaline solution environment accelerates the loss of coating adhesion.

In this article, the effectiveness of cathodic protection was evaluated by the results of the CP application, holiday size, crevice thickness, CO_2 content, and the

Corresponding author: Xu Chen, **E-mail:** cx0402@yahoo.cn
Also available online at www.sciencedirect.com

condition of steel surfaces in the chemical and electrochemical environment.

2. Experimental

2.1. Materials and solution

The working electrodes were cut from samples of X70 pipe steel. Its material composition is shown in Table 1. All test solutions were composed of the lixivium of soil. The pH of the solution was 4.6, the conductivity was 0.28 mS/cm, and the composition is listed in Table 2.

Table 1. Composition of X70 steel wt%

C	Si	Mn	S	Cr	P	Ni	Mo	Cu	Nb	Fe
0.0450	0.2400	1.4800	0.0001	0.0310	0.0170	0.1600	0.2300	0.2100	0.0330	Bal.

Table 2. Physical and chemical parameters of soil (25°C) wt%

Cl^-	SO_4^{2-}	HCO_3^-	NO_3^-	Na^+	Mg^{2+}	K^+	Ca^{2+}
0.0036	0.0018	0.0011	0.0030	0.0017	0.0002	0.0006	0.0008

2.2. Crevice cell

The crevice cell consisted of a 33.5 cm×7.5 cm×1 cm Lucite, which simulated the coating. A rectangle thermoplastic shim was used to create the crevice (Fig. 1). The thickness of plastic shim was either 0.24 mm or 0.9 mm, which controlled the thickness of the crevice between the simulated coating and the steel. An opening of either 3.5 cm×1 cm or ϕ6 mm diameter was made at 4 cm from one end of the board, which served as a holiday. The sizes were dependent upon the experiment conducted. Three ports through the Lucite block were drilled at 5 cm interval from the holiday. These ports helped to position the microelectrodes, which were used to measure the potential of the steel plate, as well as the pH and oxygen content of the crevice solution. A chamber filled with solution was assembled at the end of the Lucite board and above the holiday. The reference electrode (saturated calomel electrode, SCE) and counter electrode (Pt) were placed inside the chamber.

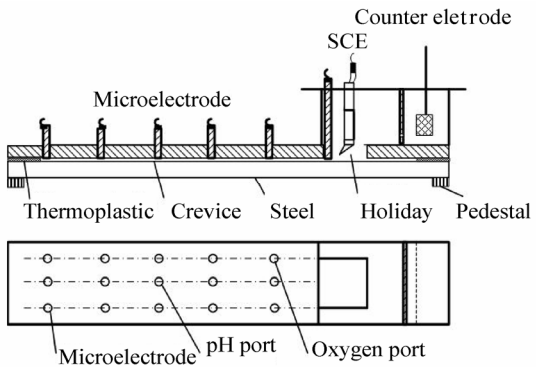

Fig. 1. Cell used to simulate a crevice under a disbonded coating.

2.3. Measurements of pH and oxygen concentration

A commercially available needle-like pH electrode and a dissolved oxygen microglass electrode were used in the experiments. Both were pierced into the ports on the Lucite to carry out measurements in site.

2.4. Electrochemical measurement

Potentialdynamic measurements were recorded with an EG&G Instrument Model 2273. During the measurements, the typical three-electrode method was used. The scan rate was 1 mV/s ranging from −1.2 V to 0.4 V *vs.* SCE. The solutions were purged with N_2 for 1 h before the potential dynamic scanned. The specimen was kept at −1.3 V *vs.* SCE for 3 min while submerged in the solutions to ensure that the oxide film was removed.

2.5. Bubbling CO_2 test and pre-corrosion test

The effect of CO_2 on the crevice corrosion of X70 steel under the coating was investigated. CO_2 was introduced into the experimental solution through purging it with 5vol% CO_2 and 95vol% N_2. The crevice corrosion was evaluated by measuring the potential distribution and pH within the crevice when the CP was applied. The effects of rust on the chemical and electrochemical environment were studied, however, the CP was not turned off. To create a crevice cell, the solution within the crevice was first evaporated to form the brown rust. Then, the soil lixivium was refilled.

All the processes listed above were carried out at room temperature. All potentials were measured against the SCE.

3. Results

3.1. Effect of applied cathodic potential (E_{cp})

The effect of applied potential on the local solution environment under the disbonded coating was investigated at three potential levels of −775, −1000, and −1200 mV with a crevice thickness of 0.9 mm and a holiday size of 3.5 cm×1 cm. The oxygen content in the solution was 8.3 mg/L.

(1) At −775 mV

The applied potential of –775 mV was measured by the microelectrodes placed along the crevice. The potential *vs.* time profile is shown in Fig. 2(a). The potential at the holiday reached –775 mV quickly and all the other positions which were 5 cm interval from the holiday were stable after 12 h. The difference of the potential in the crevice was slight. The changes of pH (Fig. 2(b)) and oxygen concentration (Fig. 2(c)) within the crevice were also recorded. The pH reached a level of 10 at the holiday, 5 cm, 10 cm, and 15 cm positions. However, the pH was 7 at the 25 cm position. The oxygen concentration at the solution-iron interface decreased rapidly.

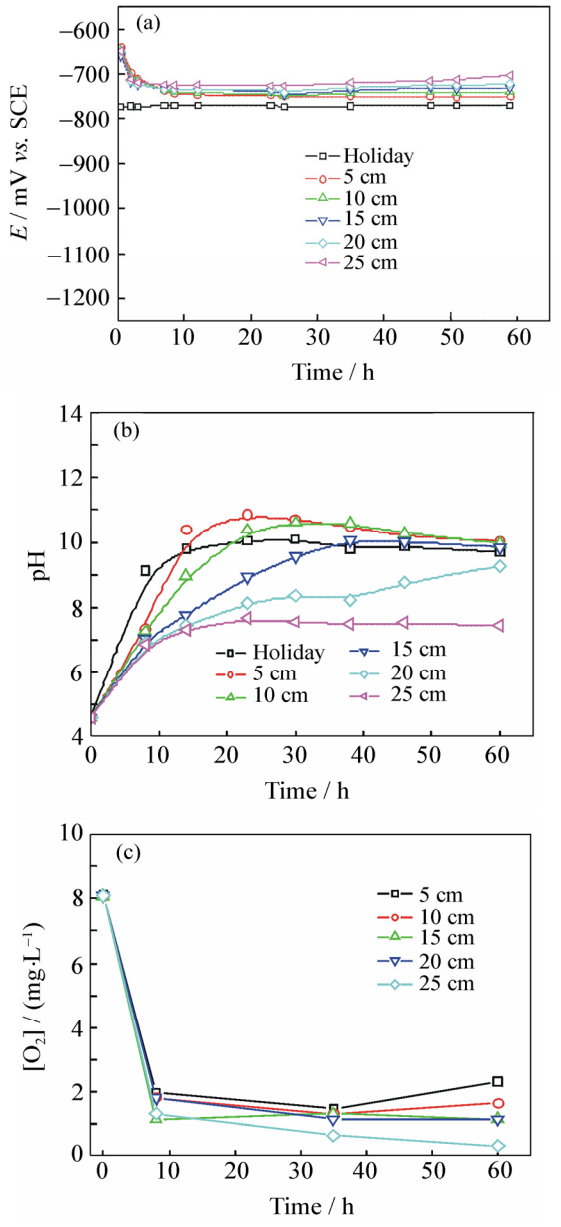

Fig. 2. Parameter curves of the steel along crevice area *vs.* time for E_{cp} = –775 mV *vs.* SCE with a crevice thickness of 0.9 mm and a holiday size of 3.5 cm×1 cm: (a) potential (*E*); (b) pH; (c) oxygen concentration.

(2) At –1000 mV

As shown in Fig. 3, The level of polarization decreased with the crevice depth increasing. The potential gradient within the crevice reduced with the time change. In order to study the effects of no CP in the crevice, the protected potential was turned off after the experiment was run for 58 h. This increased the potential of the holiday to the maximum positive level, while the potential of the crevice bottom was the most negative. This demonstrated that the speed of increasing potential was the fastest at the holiday. The initial potential distribution trend was recovered when the cathodic potential turned on again after being off for 61 h, and the potential gradient along the crevice increased slightly.

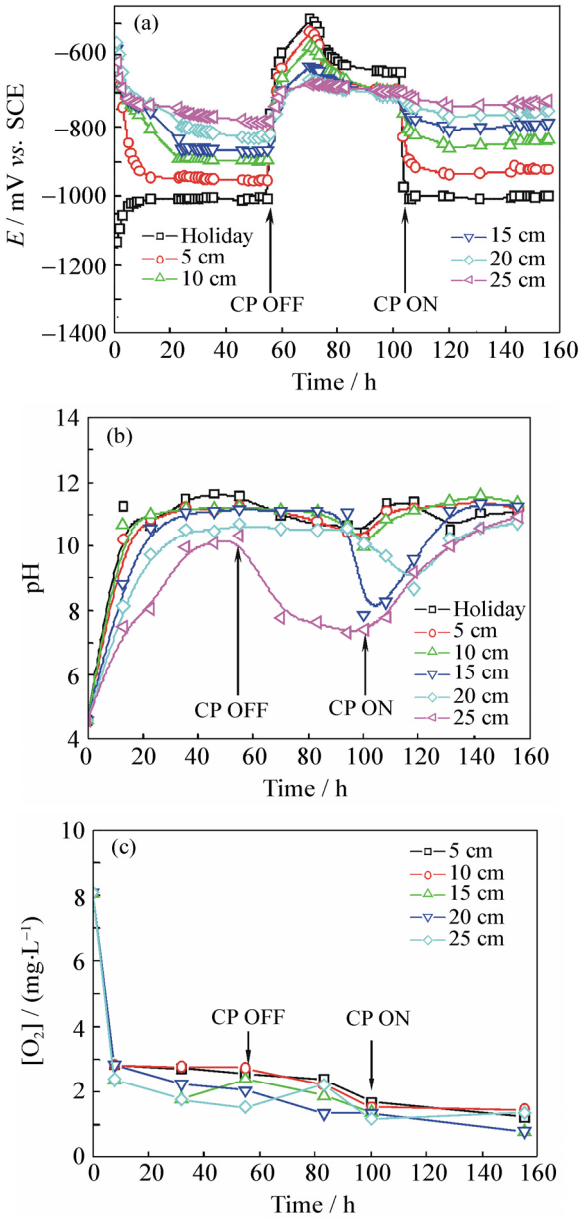

Fig. 3. Parameter curves of the steel along crevice area *vs.* time for E_{cp} = –1000 mV *vs.* SCE with a crevice thickness of 0.9 mm and a holiday size of 3.5 cm×1 cm: (a) potential (*E*); (b) pH; (c) oxygen concentration.

The pH values at various positions are shown in Fig. 3(b). For 12 h, the pH levels increased steadily,

though the pH changed at the crevice bottom lagged behind. After 12 h, the pH near the crevice mouth stabilized, but that of the crevice bottom continually increased for up to 60 h. During the time that the CP was turned off, the pH at both the 25 cm port and the holiday dropped by approximately 4 units. When the CP was turned on again, the pH returned to its former level. Fig. 3(c) shows the oxygen concentration recorded simultaneously. The oxygen concentration in the crevice decreased quickly and it was hardly affected when the CP was off.

(3) At −1200 mV

Many small bubbles were generated at the holiday, 5 cm, and 10 cm crevices when the applying potential was at −1200 mV. Fig. 4(a) shows the potential *vs.* time graph. It was noted that the potential of the holiday dropped below −1300 mV. The potential in the crevice fluctuated owing to the generation of hydrogen. The pH values at various positions are shown in Fig. 4(b). The pH of the crevice bottom increased rapidly, but the pH distribution in the crevice was uniform. The oxygen content (Fig. 4(c)) was similar to those of the −775 and −1000 mV applied potential.

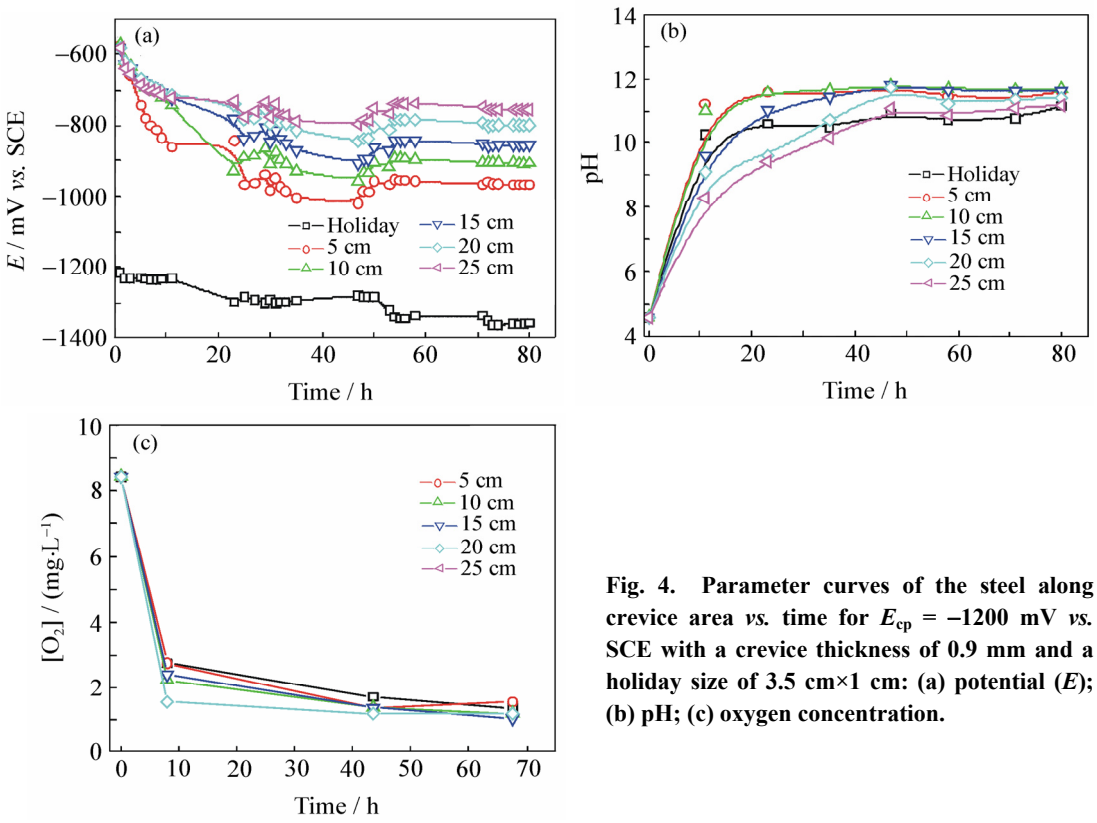

Fig. 4. Parameter curves of the steel along crevice area *vs.* time for E_{cp} = −1200 mV *vs.* SCE with a crevice thickness of 0.9 mm and a holiday size of 3.5 cm×1 cm: (a) potential (*E*); (b) pH; (c) oxygen concentration.

3.2. Thinner crevice

Fig. 5(a) shows the distribution of the potential between the 0.24 mm crevice which has the −1000 mV cathodic protection potential and the 3.5 cm×1 cm holiday. It was clear that a superior polarization level directly correlated with a thicker crevice. Except for the 5 cm position, there was hardly any potential gradient within the other crevices. The potential of all the positions above 5 cm remained at a polarization level that was nearly equal to the 25 cm position. The potential of 5 cm was more positive than that of the thicker crevice. The pH within the 0.24 mm crevice (Fig. 5(b)) increased rapidly at a slightly faster pace than within the 0.9 mm crevice. The oxygen content of the thinner crevice is shown in Fig. 5(c). The amount of oxygen within the bottom of the thinner crevice was slightly lower than that in the bottom of the thicker crevice.

3.3. Smaller size holiday

In order to study the effects of various holiday sizes on the environment under the disbonded coating, a 6 mm diameter hole was created and served as the holiday with the −1000 mV cathodic potential and the 0.9 mm crevice thickness. Both the potential gradient (Fig. 6(a)) and the polarization level of the smaller holiday decreased in comparison to that of the larger holiday. The pH (Fig. 6(b)) was more uniform and achieved stability faster than that at the larger holiday. The oxygen content (Fig. 6(c)) was found to be reduced within the larger holiday crevice.

3.4. Bubbling CO_2

It is well known that soil contains carbon dioxide from decaying organic matters. Thus, it is not surpris-

ing that the solution found within the vicinity of pipelines contains carbon dioxide related species. Fig. 7(a) shows the potential measurement results. The potential at the holiday decreased to −1000 mV. All other crevice potentials remained essentially static at −710 mV. The CP was turned off after 60 h and the results compared to the previous experiments. Again, the potential at the holiday increased positively. However, the others remained at approximately the same value. Fig. 7(b) displays the corresponding pH distribution. The crevice obtained pH of 7, but in the holidays only obtained a pH of 6 throughout the entire experiment. Turning the CP off had no effect on the pH.

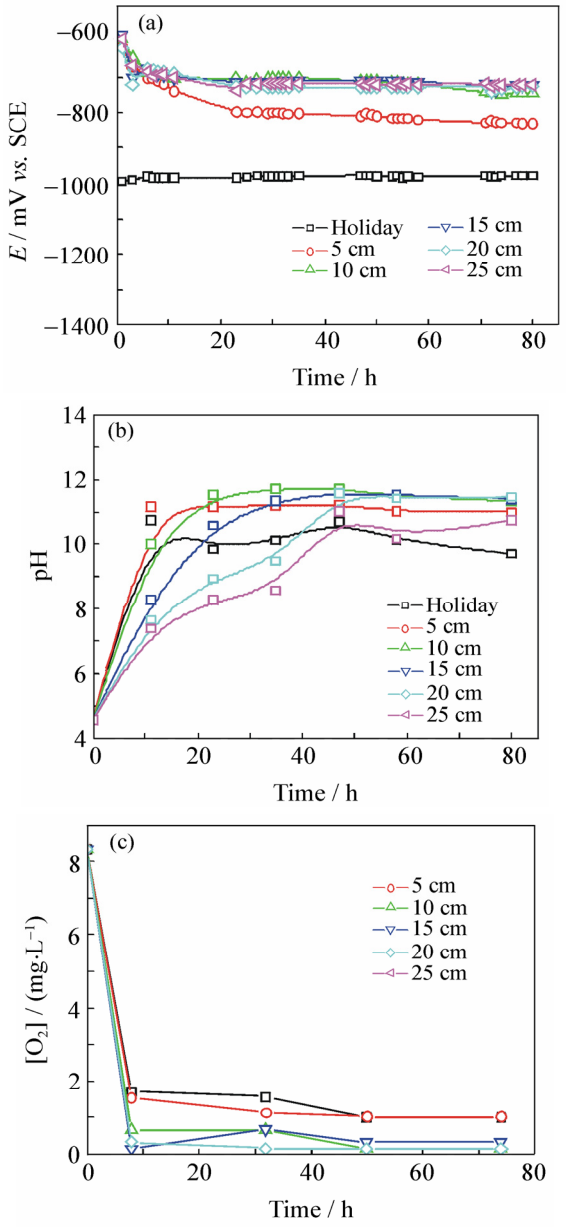

Fig. 5. Parameter curves of the steel along crevice area *vs.* time for E_{cp} = −1000 mV *vs.* SCE with a crevice thickness of 0.24 mm and a holiday size of 3.5 cm×1 cm: (a) potential (*E*); (b) pH; (c) oxygen concentration.

3.5. Pre-corrosion steel surface

During the dry season, water which is trapped underneath the disbanded coating can vaporize and hence create rust upon the steel surfaces of the pipes. During the wet season, the soil lixivium is saturated with water and seeps underneath the disbonded coating. Fig. 8(a) shows the distribution of the potential. The potential on the pre-corrosion steel advanced at a slower pace than that of the bare steel. Furthermore, the potential gradient within the crevice was diminished. The acidic level of all conditions tested rapidly increased to a pH of over 10, while the oxygen content was relatively small.

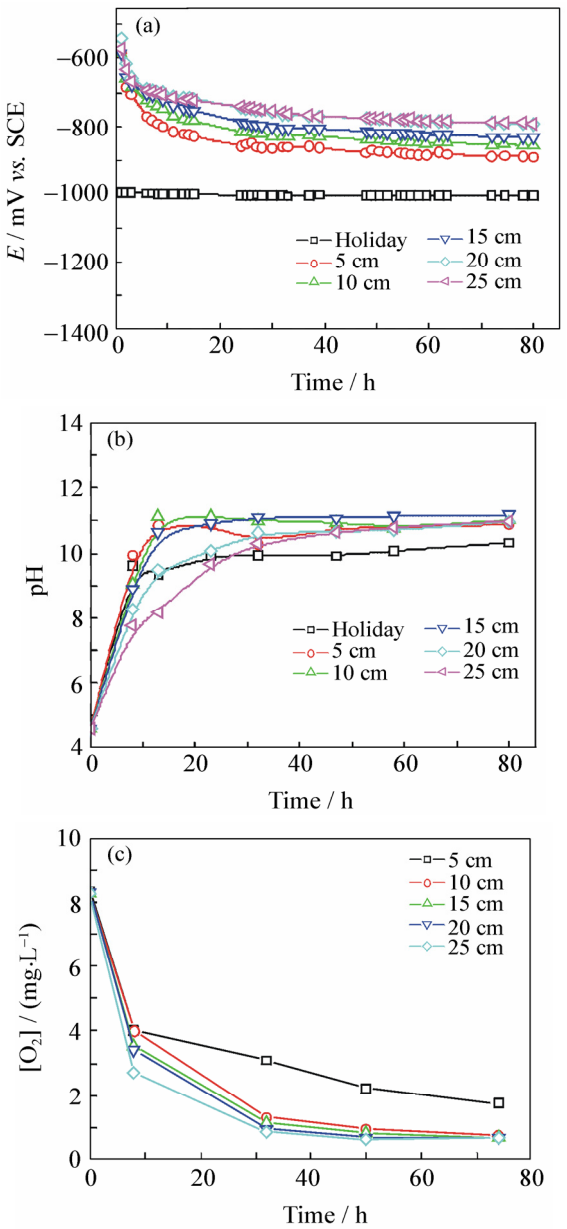

Fig. 6. Parameter curves of the steel along crevice area *vs.* time for E_{cp} = −1000 mV *vs.* SCE with a crevice thickness of 0.9 mm and a holiday size of ϕ0.6 mm: (a) potential (*E*); (b) pH; (c) oxygen concentration.

3.6. Polarization curves

The oxygen content was low and the pH ranged from 7 to 11 within the crevice. A set of polarization measurement was carried out to characterize the elec-

trochemical behavior of the X70 steel. The results are shown in Fig. 9. Deaeration and alkalinity caused the open cell potential of the steel to become more negative. When the pH was reached 9, the anode curve indicated passivation. The passivation range widened with the pH increasing.

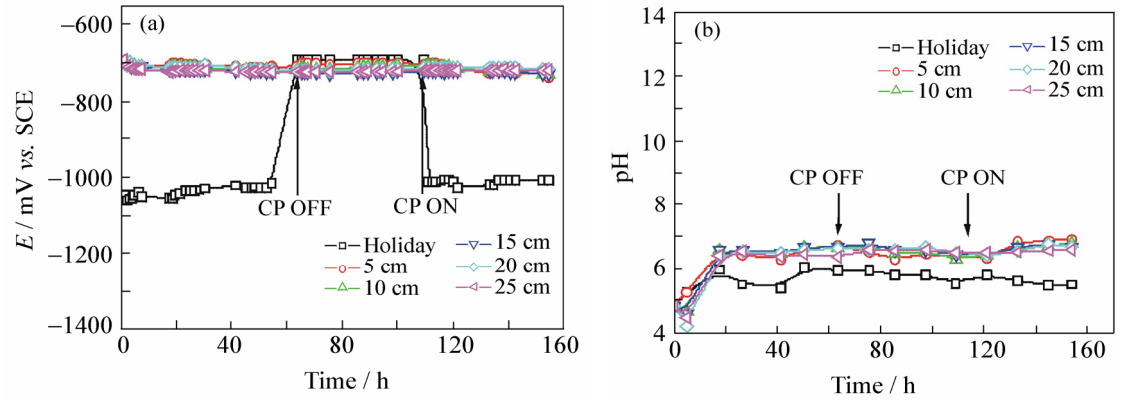

Fig. 7. Parameter curves of the steel along crevice area *vs.* time for E_{cp} = –1000 mV *vs.* SCE with a crevice thickness of 0.9 mm and a holiday size of 3.5 cm×1 cm in 5vol% CO_2+95vol% N_2 condition: (a) potential (*E*); (b) pH.

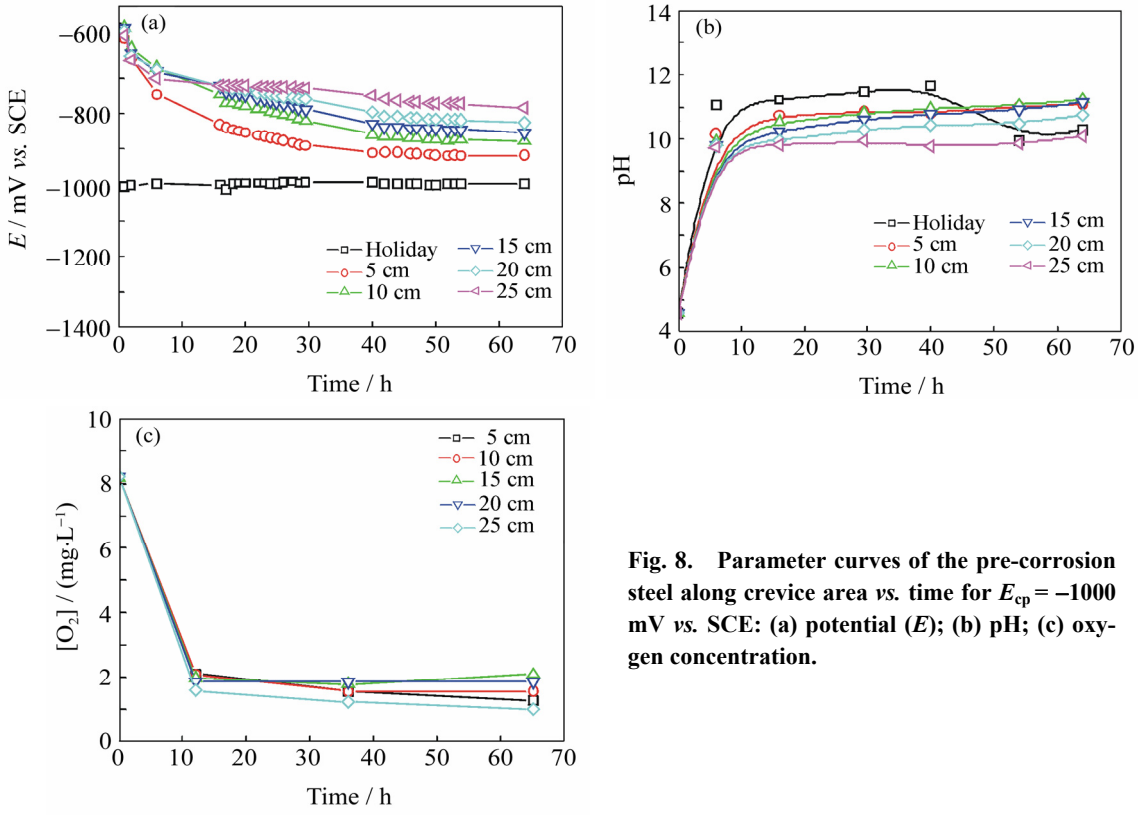

Fig. 8. Parameter curves of the pre-corrosion steel along crevice area *vs.* time for E_{cp} = –1000 mV *vs.* SCE: (a) potential (*E*); (b) pH; (c) oxygen concentration.

4. Discussion

4.1. Potential distribution

In this study, the cathodic protection potentials were –775, –1000, and –1200 mV, which were insufficient, moderate, and over the protection level, respectively. Regardless of the position, the polarization degree always increased with the more negative applied potentials.

The potential of –775 mV was the cathodic protection potential that the National Association of Corrosion Engineers (NACE) recommended for carbon steel. However, the conductivity of the soil lixivium was so low that the cathodic current could not reach the crevice bottom owing to the potential (IR) drop. According to the polarization curves, it was both oxygen depletion and the alkaline environment that were responsible for the anode dissolution condition of the steel within the crevice. The solution within the crevice was observed green when the experiments were completed. While the applied potential increased to –1200 mV, there were a number of bubbles forming at the holiday from hydrogen reduction. The bubbles blocked the cathodic current flow into the crevice, which resulted in the potential at the crevice bottom to be less than –900 mV.

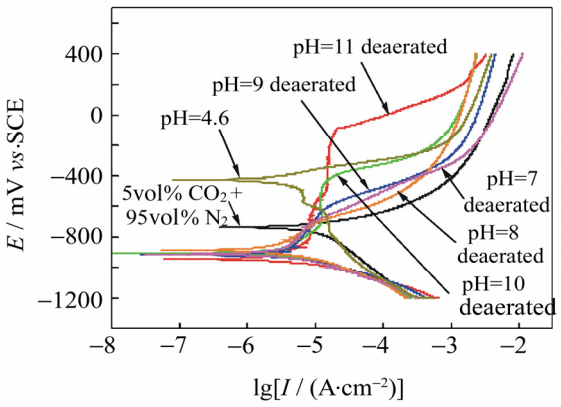

Fig. 9. Polarization curves of X70 steel at different pH valuse.

The potential results in the crevice were attributed to the higher oxygen content in the solution at the initial stage. When the steel was polarized cathodically, the thermodynamically favored electrode reaction was O_2 reduction.

$$O_2+2H_2O+4e \rightarrow 4OH^- \quad (1)$$

This electrochemical process led to the oxygen concentration difference between the crevice and the holiday. The rate at which oxygen diffused from the holiday to the crevice was considerably slower than the chemical reaction. Thus, oxygen diffusion was the control step. The difference in oxygen concentration coupled with the high resistance of the solution within the crevice resulted in the potential gradient. The higher applied potential was caused by H_2, which was formed from the following reaction:

$$2H_2O+2e \rightarrow 2OH^-+H_2 \quad (2)$$

The potential gradient ranged from 30 mV with an applied potential of −775 mV to up to more than 200 mV with an applied potential of −1200 mV. There was no other cathodic current that could flow into the crevice when the CP was off. Though the potential at the holiday immediately increased to almost 500 mV, the potential at the crevice bottom remained continuous. This distribution of the potential gradient illustrated that the crevice bottom was more negative than the holiday. This was a direct result of the polarization within the crevice created by the oxygen concentration difference within the cell. It created a current flow from the crevice bottom to the holiday. The polarization was weakened by the applied current when the CP was on.

4.2. pH change during cathodic protection

The steel in the crevice was in the anode dissolution condition with applying −775 mV. Though reaction (1) was expected in the cathodic filed, the steel as an anode can also be oxidized.

$$Fe \rightarrow Fe^{2+}+2e \quad (3)$$

Reaction (3) can produce a chemical reaction of hydrolysis, which is often referred to as the acidification reaction in crevice corrosion [15].

$$H_2O+Fe^{2+} \rightarrow FeOH^++H^+ \quad (4)$$

The steel was passivated and under the protected potential as the result of the alkaline environment formed when it shifted to a more negative potential. However, the hydrogen evolution reaction occurred and the pH increased when the applying potential was −1200 mV. The higher pH in the crevice accelerated the degradation of the coating and served as a representation of the conditions during the dry season.

Initially, the pH increased rapidly, and then it gradually leveled off. The pH in the crevice correlated to the oxygen content owing to the presence of hydroxyl ions (OH^-) generated from the oxygen reaction. It was difficult for the oxygen to diffuse into the crevice, and this concentration difference created the pH gradient. The oxygen reaction at the crevice bottom occurred at a slower rate; therefore the pH at the crevice bottom was lower than that in the holiday. Moreover, the anode dissolution process was almost completely inhibited under the cathodic polarization. Under the condition, the hydrolyze reaction that generated H^+ on the steel could not occur. At the same time, a cathodic reduction reaction can be expected in the negative electric field [14] as

$$O_2+4H^++4e \rightarrow 2H_2O \quad (5)$$

Turning the CP off had remarkable effects on the solution environment within the crevice. When the cathodic current was turned off, reaction (1) stopped. The ions in the solution diffused under the influence of the concentration gradient, and OH^- diffused out of the crevice. The steel potential within crevice was within the anode region, and thus local corrosion occurred. Ferrous hydrolyzation caused the pH decrease within the crevice.

4.3. Effect of crevice thickness

Both 0.24 and 0.9 mm crevices were studied for E_{cp} = −1000 mV *vs.* SCE for a 3.5 cm×1 cm holiday. It could be seen from the above experimental data that the polarization level inside the thinner crevice was considerably lower than that within the thicker one. However, the rate of pH increase was accelerated. This was owing to the limited solution volume within the thinner crevice and the diminished oxygen content. O_2 was rapidly consumed, which resulted in a large decrease in O_2 reduction kinetics [12]. Compared to the thicker one, the solute exchanging between the

crevice and outside solution was insufficient This made it difficult for the cathodic current flow to enter the crevice, and thus the anodic dissolution kinetics was increased.

4.4. Effect of holiday size

Overall, the variations of holiday size primarily affected the level of the polarization and alkalinity achieved. The measured potential gradient for the ϕ6 mm holiday was lower owing to a slower rate of oxygen diffusion into the crevice. The decrease in oxygen concentration resulted in a more uniform alkaline environment inside of the crevice. The pH of the smaller sized holiday was lower than that of the larger. Though the volume of solution remained the same, it was found that the smaller the exposed area, the lower the pH was. This was because the exposed surface was where oxygen reduction took place.

4.5. Effect of CO_2

Under the conditions with 5vol% CO_2 and 95vol% N_2, the potential in the crevice hardly changed with time. The hydroxyl ions that were derived from the cathodic potential resulted in a pH of up to 7 within the crevice at the initial stage. After the initial stage, the pH then stabilized. This indicated that there was resistance in increasing the pH past 7. The presence of CO_2 not only promoted hydrogen evolution, but also inhibited the alkaline environment. This could have resulted from the following chemical reactions [10].

Anodic:

$$Fe-2e = Fe^{2+} \quad (6)$$

Cathodic:

$$CO_2+H_2O = H_2CO_3 \quad (7)$$

$$H_2CO_3=H^++HCO_3^- \quad (8)$$

$$HCO_3^-=H^++CO_3^{2-} \quad (9)$$

$$Fe^{2+}+CO_3^{2-}=FeCO_3 \quad (10)$$

$FeCO_3$ precipitated on the steel with the form of a corrosion product film. The continuous bubbling CO_2 promoted the cathodic reaction, which led to the steel dissolution. According to the Nernst equation, the activity ratio of Fe^{2+} and CO_3^{2-} remained a constant, therefore, the potential had no change during the experiment.

There was a balance between the continual introduction of CO_2 and OH^- ions, which were derived from the cathodic reaction and their role in maintaining the pH at 7.

Turning CP off had no effect on the potential and pH inside the crevice because of the absence of the oxygen concentration gradient.

4.6. Effect of surface state

The trapped water under the disbanded coating would vaporize and rust was on the steel surface during the days of water shortage. During the rainy season, there was full soil lixivium under the disbanded coating. The level of the polarization for the pre-corroded steel surface was considerably lower than the bare steel surface because the loose corrosion products prevented the cathodic current from reaching into the crevice. The rust X-ray diffraction (XRD) showed that the FeO(OH) oxidization reaction consumed part of the available oxygen supply, and thus caused a reduction within the polarization rate. This could be proved by the metamorphosis of the red-brown rust into the black corrosion products (XRD showed Fe_3O_4). Stratmann, *et al*. [16] considered that rust was transited by the intermediate product Fe^{2+} in the acidic environment. In response, the Fe^{2+} ions can generate Fe_3O_4 in the following reaction:

$$FeO(OH)+H^++e \rightarrow Fe{\cdot}OH{\cdot}OH \quad (11)$$

$$Fe{\cdot}OH{\cdot}OH+FeO(OH) \rightarrow Fe_3O_4+2H_2O \quad (12)$$

While the pre-corroded steel was drying, the alkaline environment could not be maintained because the CP was off. This promoted the local cell reaction when oxygen entered the porous corrosion products. When the acid solution was filtered off from the crevice again, the pH increased rapidly (pH = 11) by the use of reactions (1) and (11). This revealed that the cathodic reaction within the crevice still reduced oxygen first. This proposition was also supported by the oxygen content measurement. In the alkaline environment, the majority of the oxygen that diffused into the crevice took part in the rust oxidization reactions in succession, and thus resulted in a constant pH within the crevice.

5. Conclusions

(1) The cathodic protection potential for X70 steel in the acidic soil environment is –1000 mV *vs.* SCE or more negative. The potential within the crevice drops and the available protection distance increases with the negative shift of the applying potential.

(2) The steady local solution environment is obtained easily in the thinner crevice, but the polarization level at the crevice bottom is insufficient.

(3) The presence of CO_2 inhibits the formation of the alkaline environment, which leads to the near-neutral pH inside the crevice.

(4) The rust layer on the steel reduces the polarization speed. The pH increases rapidly and is stabilized because of the porosity of the rust layer.

(5) The cathodic protection potential notably changes the chemical and electrochemical characteristics of the ground water solution under the disbonded coating. The transformation processes experienced under different conditions inside the crevice are accordant. These processes include potential decreasing, pH increasing, and oxygen exhaustion.

References

[1] D.T. Chin and G.M. Sabde, Modeling transport process and current distribute in a cathodically protected crevice, *Corrosion*, 56(2000), No.8, p.783.

[2] J.A. Bervers and N.G. Thompson, Corrosion beneath disbonded pipeline coatings, *Mater. Perform.*, 36(1997), No.4, p.13.

[3] M. Puiggali, S. Rousserie, and M. Touzet, Fatigue crack initiation on low-carbon steel pipes in a near-neutral-pH environment under potential control conditions, *Corrosion*, 58(2002), No.11, p.961.

[4] Y.Q. Song, C.W. Du, and X.G. Li, Electrochemical corrosion behavior of carbon steel with bulk coating holidays, *J. Univ. Sci. Technol. Beijing*, 13(2006), No.2, p.37.

[5] F.M. Song, D.A. Jones, and D.W. Kirk, Predicting corrosion and current flow within a disc crevice on coated steels, *Corrosion*, 61(2005), No.2, p.145.

[6] E. Gamboa, V. Linton, and M. Law, Fatigue of stress corrosion cracks in X65 pipeline steels, *Int. J. Fatigue*, 30(2008), No.5, p.850.

[7] M.C. Yan, J.Q. Wang, and E.H. Han, Local environment under simulated disbonded coating on steel pipelines in soil solution, *Corros. Sci.*, 50(2008), No.5, p.1331.

[8] P.G. Fazzini and J.L. Otegui, Experimental determination of stress corrosion crack rates and service lives in a buried ERW pipeline, *Int. J. Pressure Vessels Piping*, 84(2007), No.12, p.739.

[9] B.A. Harle and J.A. Beavers, Technical note: low-pH stress corrosion crack propagation in API X-65 carbon steel in dilute aqueous solution, *Corrosion*, 50(1994), No.5, p.334.

[10] M.C. Li and Y.F. Cheng, Mechanistic investigation of hydrogen-enhanced anodic dissolution of X-70 pipe steel and its implication on near-neutral pH SCC of pipelines, *Electrochim. Acta*, 52(2007), No.28, p.8111.

[11] D.T. Chin and G.M. Sabde, Current distribution and electrochemical environments in a cathodically protected crevice, *Corrosion*, 55(1999), No.3, p.229.

[12] J.J. Perdomo, M.E. Chabica, and I. Song, Chemical and electrochemical conditions on steel under disbonded coatings: the effect of previously corrosion surface and wet and dry cycles, *Corros. Sci.*, 43(2001), No.3, p.515.

[13] N. Sridhar, D.S. Dunn, and M. Seth, Application of a general reactive transport model to predict environment under disbonded coating, *Corrosion*, 57(2001), No.7, p.598

[14] S. Szabó and I. Bakos, Impressed current cathodic protection, *Corros. Rev.*, 24(2006), No.1, p.39.

[15] J.J. Perdomo and I. Song, Chemical and electrochemical conditions on steel under disbonded coatings: the effect of applied potential, solution resistivity, crevice thickness and holiday size, *Corros. Sci.*, 42(2000), No.8, p.1389.

[16] M. Stratmann, K. Bohnenkamp, and H.J. Engell, An electrochemical study of phase-transitions in rust layers, *Corros. Sci.*, 23(1983), No.9, p.969.